Journal of
Synchrotron Radiation

ISSN 0909-0495

Received 4 August 2006
Accepted 21 September 2006

Ion distributions at charged aqueous surfaces by near-resonance X-ray spectroscopy

Wei Bu, Philip J. Ryan and David Vaknin*

Ames Laboratory, and Department of Physics and Astronomy, Iowa State University, Ames, IA 50011, USA. E-mail: vaknin@ameslab.gov

Near-resonance X-ray spectroscopy is used to determine ion distributions and their local environment at charged aqueous interfaces. Energy scans at fixed momentum-transfers under specular reflectivity conditions near the L_{III} Cs^+ resonance reveal the formation of a diffuse Gouy–Chapman layer at a charged surface formed by a Langmuir monolayer (dihexadecyl phosphate) spread on CsI solution. The energy scans exhibit a periodic dependence on photon momentum-transfer (Q_z) with a line-shape that consists of a Q_z-dependent linear combination of the dispersive $f'(E)$ and absorptive $f''(E)$ fine-structure corrections. The results in the Born approximation are discussed and more quantitatively by using the dynamical method numerically (*i.e.* recursive or matrix methods to calculate the reflection of electromagnetic waves from stratified media). The ion distributions obtained from the analysis of the spectroscopy are in excellent agreement with those obtained from anomalous reflectivity measurements, providing further confirmation to the validity of the renormalized surface-charge Poisson–Boltzmann theory for monovalent ions. The fine structures of $f'(E)$ and $f''(E)$ obtained in the process differ significantly from the multi-electron photoexcitation spectra of the isolated ion, revealing the local environment of a Cs^+ ion in the solution at the interface. The comparison with similar X-ray absorption fine structures suggests that the Cs^+ ion is surrounded by a shell of eight O atoms.

Keywords: XAFS of Cs in aqueous environment; f' and f'' anomalous terms for Cs ions; electrostatics in aqueous solutions; charged membranes; interfacial Possion–Boltzmann theory.

1. Introduction

Theoretical predictions of ion distributions at charged surfaces were first provided by Gouy (1910) and Chapman (1913) who employed the Poisson–Boltzmann (PB) theory. Indirect experimental verification of PB theory came from radio-tracing measurements by Tajima (1971), and electro-kinetic and visco-electric effects studies (Hunter, 1981; McLaughlin, 1989). Subsequent force measurements that can be converted to the spatial dependence of potential showed good agreement with PB theory at distances larger than $\sim$20 Å from the charged surface (Israelachvili, 2000). More recently, modulated infrared spectroscopy (LeCalvez *et al.*, 2001) and surface-sensitive X-ray scattering techniques (Kjaer *et al.*, 1989; Bloch *et al.*, 1988; Bedzyk *et al.*, 1990; Vaknin *et al.*, 2003; Bu *et al.*, 2005; Luo *et al.*, 2006) from charged interfaces revealed quantitatively the interfacial accumulation of ions in the vicinity of the charged head-group region.

Herein we report experimental determination of monovalent ion distributions (Cs^+) at highly charged interfaces using energy scans at fixed momentum-transfers under specular-reflectivity conditions and compare these findings with recent results using the anomalous reflectivity technique (Bu *et al.*, 2005, 2006). As shown below, our analysis also yields the energy dependence of the dispersion corrections of Cs^+, $f'(E)$ and $f''(E)$, near a resonance, which we find shed light on the local environment of the non-crystalline ions. In the past, such corrections were obtained by Bijvoet pairs at Bragg reflections (Templeton *et al.*, 1980), by absorption cross-section measurements (Kemner *et al.*, 1996; Gao *et al.*, 2005), and by calculation using atomic wavefunctions (Cromer & Libermann, 1970). Our independent findings resemble recent near-resonance reflectivity and spectra at the Pt L_{III}-edge of platinum tetra-amine at the quartz–water interface (Park *et al.*, 2005).

2. Experimental details

To form interfacial charges, monolayers of dihexadecyl hydrogen phosphate (DHDP) were spread at CsI solution/gas interfaces (Gregory *et al.*, 1997, 1999). Detailed procedures of sample preparations and handling have been described by Bu

et al. (2005, 2006). *In situ* X-ray studies at the gas/liquid interface were conducted on the Ames Laboratory liquid-surface diffractometer at the Advanced Photon Source, beamline 6ID-B [described elsewhere (Vaknin, 2001)]. The highly monochromatic X-ray beam, selected by a downstream Si double-crystal monochromator, is deflected onto the liquid surface at a desired angle of incidence with respect to the liquid surface by a second monochromator [Ge(111) or by a *y*-cut quartz single crystal; *d*-spacings 3.266368 and 4.25601 Å, respectively] mounted on the liquid-surface diffractometer yielding an energy resolution of ~0.85 eV in the vicinity of the Cs^+ L_{III} resonance (~5 keV). The absolute scale of the X-ray energy was calibrated with various absorption edges to better than ±2 eV. The incident photon energy can be continuously varied from ~4 to 40 keV, in a fixed-Q mode, namely adjusting all angles to maintain fixed momentum-transfer. Scattered photon intensities are normalized to an incident beam monitor in front of the sample.

Specular X-ray reflectivity techniques have been commonly used to determine the electron-density profiles across stratified interfaces. We recently described in detail how to extract the generalized complex density profile, $\rho(z, E) = \rho' + i\rho''$ (z-axis is normal to the interface), of the electron density (ED) and the absorption density (AD), real and imaginary parts, respectively (Bu *et al.*, 2005, 2006). The generalized density relates directly to atomic constituents by

$$\rho(z, E) = \sum_j N_j(z)\, Z_j\, f_j(E), \qquad (1)$$

where E is the X-ray photon energy, N_j is the number density of an atomic constituent of type j with Z_j electrons, and $f_j(E)$ is the atomic form factor,

$$f(E) = f^0(Q_z) + f'(E) + if''(E), \qquad (2)$$

consisting of a photon-energy-independent term [$f^0(Q_z) \simeq 1$ for small-angle scattering and reflectivity experiments] and real and imaginary corrections near atomic binding energies. The dispersion corrections are related through the Kramers–Kronig relation (James, 1948). The reflectivity can be calculated from the complex function refractive index,

$$n(z, E) = 1 - r_0 \rho(z, E)\lambda^2/2\pi, \qquad (3)$$

where r_0 is the classical electron radius and λ is the X-ray wavelength.

3. Results and discussion

Fig. 1 shows normalized reflectivity curves, R/R_F *versus* Q_z, for DHDP (surface pressure π = 40 mN m^{-1}) spread on 10^{-3} M CsI solution measured at and off the Cs L_{III} resonance (at 5.012 keV and at 16.2 keV, respectively; R_F is the calculated reflectivity of an ideally flat gas/water interface). The minima of the reflectivity measured at the Cs resonance are slightly shifted to larger Q_z, suggestive of a smaller effective film thickness compared with that measured off resonance. This is due to the reduction in the effective number of electrons near the resonance (Vaknin *et al.*, 2003), which is also responsible for the overall intensity reduction compared with that measured away from the resonance. As described in more detail elsewhere (Bu *et al.*, 2005, 2006), the generalized density $\rho(z)$ can be extracted from the two reflectivities as shown in Fig. 2 for $\rho'(z)$. From the difference between the two EDs obtained at two energies we can quantify the spatial distribution of Cs^+ at the interface. It has been shown that this distribution is in good agreement with the renormalized-surface charge density Poisson–Boltzmann theory after convolution with the experimental resolution function, as shown in Fig. 2 (Ninham & Parsegian, 1971; Bu *et al.*, 2005, 2006).

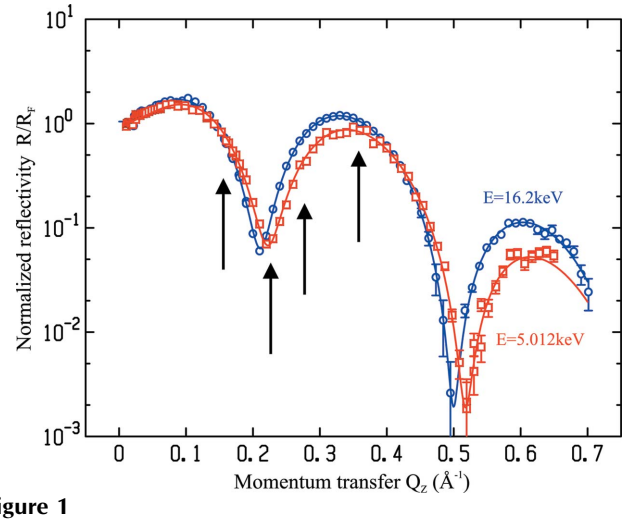

Figure 1
Normalized X-ray reflectivities measured at 16.2 keV (circles) and 5.012 keV (squares) of a DHDP monolayer spread on 10^{-3} M CsI solution (π = 40 mN m^{-1}). Arrows indicate the selected momentum transfers at which energy scans were measured. Solid lines are best fits to the data.

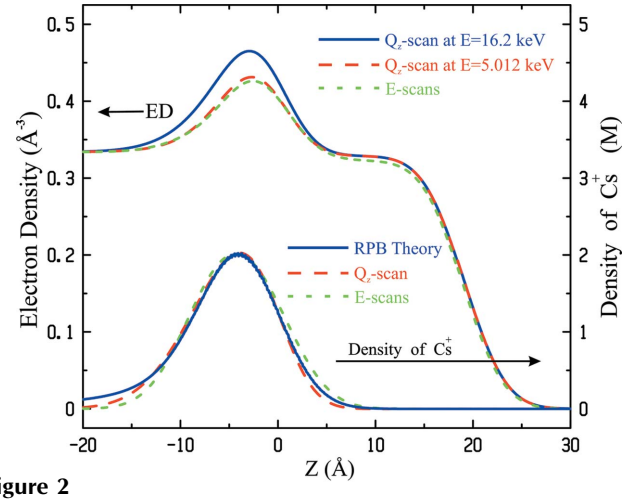

Figure 2
Electron densities obtained from the reflectivities shown in Fig. 1 at 16.2 keV and 5.012 keV, and from the combined energy scans shown in Fig. 3 also calculated at the resonance. Spatial Cs^+ distributions determined from the reflectivity measurements (dashed line) and energy scans (dotted line). The solid line is obtained from renormalized surface-charge PB theory after convolution with the experimental resolution function (Bu *et al.*, 2005, 2006). Z = 0 is defined, arbitrarily, at the interface between the head-group and the hydrocarbon chain.

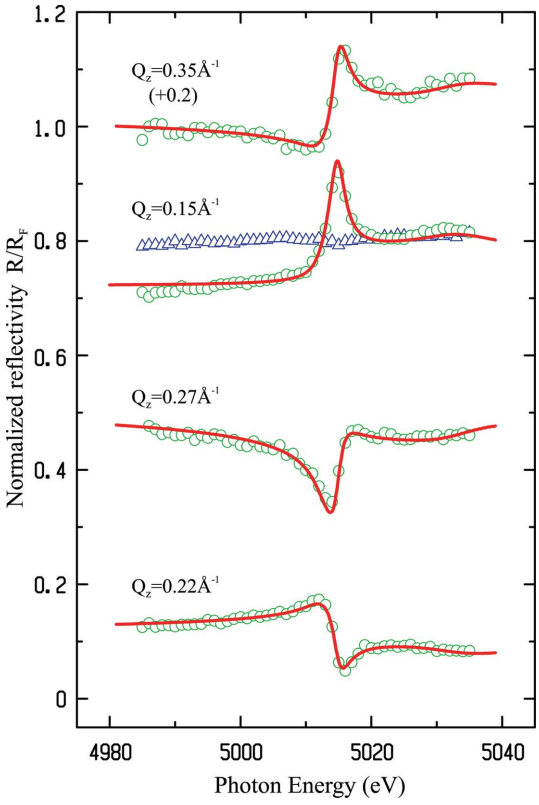

Figure 3
Energy scans at fixed momentum-transfers Q_z (as indicated by arrows in Fig. 1) near the Cs L_{III}-edge of a DHDP monolayer spread on 10^{-3} *M* CsI solution ($\pi = 40$ mN m^{-1}). Solid lines are best fits to the data as described in the text (energy scan at $Q_z = 0.35$ Å^{-1} is offset vertically, by +0.2, for clarification). Energy scans of the CsI solution surface (10^{-3} *M*) at $Q_z = 0.15$ Å^{-1} (triangles) do not detect any anomalies in the absence of interfacial charges, *i.e.* with no monolayer.

Fig. 3 shows normalized reflectivities (R/R_F) at fixed momentum transfer Q_z *versus* incident photon energies measured near the Cs^+ L_{III} resonance. Similar reflectivity measurements performed on the CsI solution (10^{-3} *M*, in the absence of a monolayer) did not reveal any anomalies in the reflected beam as a function of photon energy, as shown in Fig. 3 for $Q_z = 0.15$ Å^{-1} (triangles). Furthermore, we did not detect any signal in energy scans around the I^- L_{III} absorption edge (4.557 keV) at fixed Q_z. This is clear evidence that the concentration of I^- is in fact depleted with respect to that of the bulk at the interface. The DHDP monolayer containing the *R*-PO_4H head-group, with its strong proton dissociation constant ($pK_a = 2.1$), provides negative surface charges attracting a sufficient number of Cs^+ counterions giving rise to the spectra observed. Based on the experimental set-up, we estimate that the signal originates from $\sim 5 \times 10^{13}$ Cs^+ ions ($\sim 10^{-8}$ g Cs spread over 0.4 cm^2 of the beam footprint). We find that the energy scans exhibit periodic dependence on photon momentum-transfer (Q_z), with a line-shape that resembles a superposition of the dispersive $f'(E)$ and absorptive $f''(E)$ fine-structure corrections. The spectra systematically exhibit opposite characteristics for each two points separated by $\Delta Q_z \simeq 0.125$ Å^{-1}.

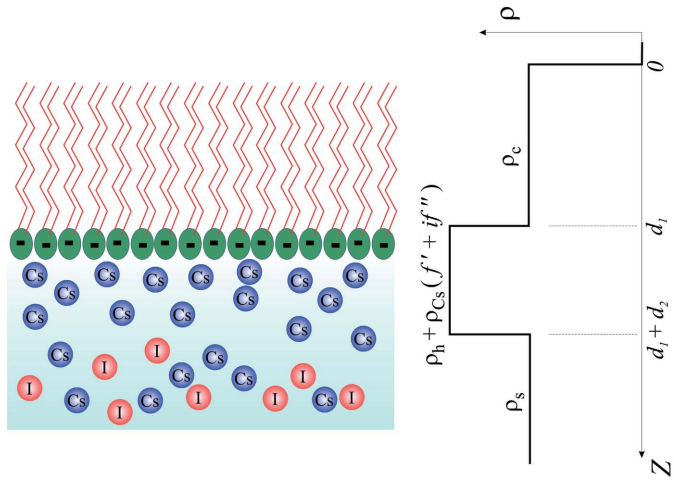

Figure 4
Simplified step-like electron-density profile used to calculate the reflectivity in the Born approximation as explained in the text.

To explain these features semi-quantitatively, we assume for simplicity that the monolayer ED consists of two slabs (as shown in Fig. 4), one of thickness d_1 and electron density ρ_c associated with the hydrocarbon chains ($\rho_c \simeq \rho_s$; the subphase ED, ρ_s, is almost the same as that of closely packed hydrocarbon chains). The second slab, of thickness d_2, is associated with the head-group and hydrated Cs^+ ion distribution ($d_2 = d_{head} + d_{Cs}$), with a complex ED, $\rho_h + \rho_{Cs}(f' + if'')$ ($\rho_{Cs} = Z_{Cs}N_{Cs}$; N_{Cs} is the number of Cs ions per molecule). In the Born approximation, the reflectivity from the film is given by (Kjaer *et al.*, 1989; Vaknin, 2001)

$$R(Q_z, E) = \frac{R_F(Q_z)}{\rho_s^2}\left|\int \frac{d\rho(z, E)}{dz}\exp(iQ_z z)\,dz\right|^2, \qquad (4)$$

valid for $Q_z \gg Q_c$, where $Q_c = 4(\pi\rho_s r_0)^{1/2} \simeq 0.0217$ Å^{-1} is the critical momentum-transfer for total reflection. Using (4) and the simplified aforementioned generalized density for the film, we obtain,

$$\begin{aligned}\frac{R(Q_z, E)\rho_s^2}{R_F(Q_z)} \simeq{}& \rho_c^2 + (\rho_h - \rho_c)^2\left[2 - 2\cos(Q_z d_2)\right] \\ &+ 4\rho_c(\rho_h - \rho_c)\sin(Q_z\bar{d})\sin(Q_z d_2/2) \\ &+ \left\{4\rho_c\rho_{Cs}\left[f'\sin(Q_z\bar{d}) - f''\cos(Q_z\bar{d})\right]\right. \\ &\left.\times \sin(Q_z d_2/2)\right\}, \qquad (5)\end{aligned}$$

where $\bar{d} = d_1 + d_2/2$. The last term in (5) predicts that a linear combination of $f'(E)$ and $f''(E)$ is superimposed on the reflectivity from the monolayer at energies away from the resonance. Furthermore, the resonant contribution of any point Q_z^j is exactly opposite in sign to any other point Q_z^i for which $(Q_z^i - Q_z^j)\bar{d} = \Delta Q_z\bar{d} = \pi$, as we observe experimentally. This property yields $\bar{d} = \pi/\Delta Q_z \simeq 25.1$ Å. Using the literature value of $d_1 \simeq 19.7$ Å (Gregory *et al.*, 1997) we obtain $d_2 \simeq 10.8$ Å corresponding to the phosphate head-group and hydrated Cs^+ compartment, which is much larger than that found for a monolayer spread on pure water, $d_2 \simeq 3.4$ Å

(Gregory *et al.*, 1997). This unequivocally demonstrates that Cs^+ ions accumulate but do not bind to the phosphate head-group at the interface, forming an extended (diffuse) layer much larger than the hypothetical bound Cs-phosphate. It is interesting to note that equation (5) counter-intuitively indicates that the absorption term f'' can enhance the reflectivity, for $Q_z\bar{d} = \pi$, as evidenced in Fig. 3 for $Q_z = 0.15$ Å^{-1}. More generally, equation (5) predicts that for $Q_z\bar{d} \simeq 3\pi/2$ or $5\pi/2$ (*i.e.* $Q_z = 0.22, 0.35$ Å^{-1}), the spectrum resembles $\mp f'_{Cs}(E)$; and if $Q_z\bar{d} \simeq \pi$ or 2π (*i.e.* $Q_z = 0.15, 0.27$ Å^{-1}) it resembles $\pm f''_{Cs}(E)$, consistent with our observations (Fig. 3).

To provide a more quantitative account of the energy scans, we employ a more accurate method to calculate the reflectivity recursively (Parratt, 1954) by slicing a parameterized generalized density profile, $\rho(z)$ (Bu *et al.*, 2005, 2006), and refining its parameters by a non-linear-squares fit method. To include the energy-dependent dispersion corrections near resonance, we construct the absorptive portion, $f''(E)$, as a sum of one error function [of known step height from the literature (Henke *et al.*, 1993)], and superimpose on it the minimum number of Lorentzians necessary to obtain an adequate fit and for which the addition of another one does not improve the quality of the fit. The dispersive portion, $f'(E)$, is numerically calculated by the Kramer–Kroning relation (integration is performed over a finite energy range using Simpson's rule). Integration by the Kramer–Kroning relation of f'' with close by anomalies ($\sim\pm$200 eV away from the Cs L_{III} resonance) did not affect the shape of f' near the resonance. To improve the reliability of the procedure, we use a single parameter set for the refinement of a combined data consisting of all energy-scans at different Q_z values. Note that the spectra shown in Fig. 3 are given on an absolute scale. The solid lines in Fig. 3 are calculated with one set of parameters that best fit the combined data set.

The generalized density profile obtained from this procedure is consistent within error with that obtained from the Q_z-scan reflectivity as shown for the ED (real part) in Fig. 2 (dotted line). As described by Bu *et al.* (2005, 2006), three energy-dependent error functions are used to construct the generalized density that best fits the spectra. The centers of the error functions define the average thicknesses of molecular compartments in the film as follows: $d_{chain} = 19.5$ Å for the hydrocarbon chains, $d_{head} = 3.0$ Å for the head-group, and $d_{Cs^+} = 7.1$ Å for the hydrated Cs^+ diffuse layer (our analysis indicates partial protrusion of Cs^+ into the head-group compartment). The combined thickness, $d_2 = d_{head} + d_{Cs^+} = 10.1$ Å, is in good agreement with that extracted from the Born approximation calculation (10.8 Å), equation (5) described above. Using these parameters we construct the ion distribution $N_{Cs^+}(z)$ (Fig. 2, dotted line), and obtain on average 0.58 integrated Cs^+ per lipid with approximately 11 water molecules in the head-group and the Cs^+ compartments. The value agrees with that obtained from the Q_z-scan reflectivity (0.56 ± 0.1) and with the renormalized-surface-charge Poisson–Boltzmann theory (Bu *et al.*, 2005, 2006).

Fig. 5 shows the dispersion corrections for Cs^+ near the L_{III}-edge extracted from the energy scans (solid lines), from the

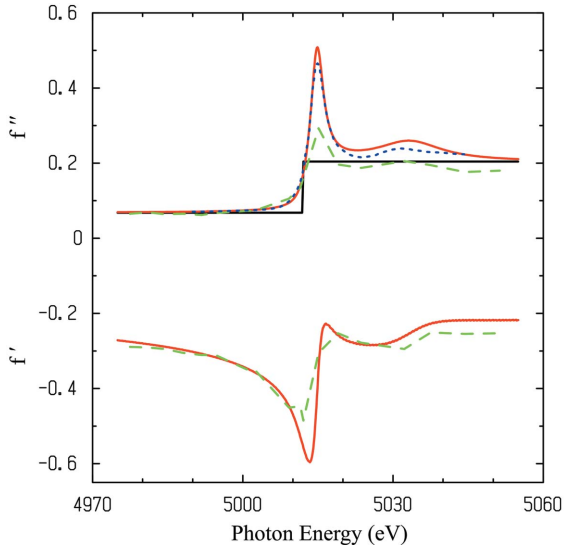

Figure 5
Dispersion corrections near the Cs L_{III}-edge. The solid lines are derived from the best fit to the spectra shown in Fig. 3. The dashed line was obtained from the Bijvoet pairs measurements of $CsHC_4H_4O_6$ single crystal (Templeton *et al.*, 1980), the dotted line was measured by absorption of $CsNO_3/H_2O$ solution (Gao *et al.*, 2005), and the step-like function was calculated by Cromer & Libermann (1970).

Bijvoet pairs in $CsHC_4H_4O_6$ single crystal (dashed line) (Templeton *et al.*, 1980), from $CsNO_3/H_2O$ solution (dotted line) (Gao *et al.*, 2005), and from the calculated step function (Cromer & Libermann, 1970). Our extraction of $f''(E)$ shows an enhanced Lorentzian at resonance (so-called white line, centered at 5013.33 ± 0.11 eV, height 0.32 ± 0.03 and width 1.49 ± 0.11 eV) and a second Lorentzian (centered at 5033.29 ± 0.19 eV, height 0.054 ± 0.003, width 7.91 ± 0.53 eV). We find that the absorption edge, defined as max(df''/dE), is at 5013.9 eV, within the uncertainty of the values of 5012 eV found in the literature (Templeton *et al.*, 1980; Kemner *et al.*, 1996; Gao *et al.*, 2005). The fine structures of $f'(E)$ and $f''(E)$ obtained in the process differ significantly from the multi-electron photoexcitation spectra of the isolated ion (Arčon *et al.*, 2005), revealing the local environment of a Cs^+ ion in the solution at the interface. Although the edge we find agrees very well with that of the single crystal $CsHC_4H_4O_6$ (Templeton *et al.*, 1980), the overall features of f' and f'' are significantly different. We argue that this is due to the fact that the local environment of Cs in the crystal consists primarily of H atoms, whereas the local environment of the ion in the present study consists of O atoms from the solution and the PO_4^- head-group. Indeed, a recent XAFS study of $CsNO_3$ in water solution (Gao *et al.*, 2005) exhibits a f'' that is very similar to the value we obtained (Fig. 5). In that study it was found that the Cs ion is surrounded by eight O atoms with six nearest water molecules at an average distance of 3.25 Å and another two at 4.0 Å (Krestov *et al.*, 1994; Gao *et al.*, 2005).

4. Summary

In the present study we demonstrated that ion distributions close to a charged surface can be extracted from reflectivity

spectra near an edge of a specific ion. This technique can be used in conjunction with fixed energy reflectivity measurements to improve the reliability of the film structural parameters. It also provides unequivocal evidence for the presence of minute ion accumulation at aqueous interfaces. This ion-specific procedure has thus the advantage of showing the depletion of certain ions at the interface; in this study they show the depletion of the co-ions I^- at the interface. Furthermore, this process is unique in providing, on an absolute scale, the dispersion corrections of a specific ion in aqueous environments. This technique is invaluable in distinguishing ion distributions from bound ions, as expected (Travesset & Vaknin, 2006; Pittler *et al.*, 2006) for multivalent ions (such as Ba^{2+} or La^{3+}) at charged interfaces.

We thank D. S. Robinson and D. Wermeille for technical support at the 6-ID beamline, and A. Travesset, C. Park and P. Fenter for illuminating discussions. The MUCAT sector at the APS is supported by the US DOE Basic Energy Sciences, Office of Science, through Ames Laboratory under contract No. W-7405-Eng-82. Use of the Advanced Photon Source is supported by the US DOE, Basic Energy Sciences, Office of Science, under Contract No. W-31-109-Eng-38.

References

Arčon, I., Kodre, A., Padežnik Gomilšek, J., Hribar, M. & Mihelič, A. (2005). *Phys. Scr.* T**115**, 235–236.
Bedzyk, M. J., Bommarito, G. M., Caffrey, M. & Penner, T. L. (1990). *Science*, **248**, 52–56.
Bloch, J. M., Yun, W. B., Yang, X., Ramanathan, M., Montano, P. A. & Capasso, C. (1988). *Phys. Rev. Lett.* **61**, 2941–2944.
Bu, W., Vaknin, D. & Travesset, A. (2005). *Phys. Rev. E*, **72**, 060501(R)/1–4.
Bu, W., Vaknin, D. & Travesset, A. (2006). *Langmuir*, **22**, 5673–5681.
Chapman, D. L. (1913). *Philos. Mag.* **25**, 475–481.
Cromer, D. T. & Libermann, D. (1970). *J. Chem. Phys.* **53**, 1891–1898.
Gao, J.-X., Wang, B.-W., Liu, T., Wang, J.-C., Song, C.-L., Chen, Z. D., Hu, T.-D., Xie, Y.-N., Zhang, J. & Yang, H. (2005). *J. Synchrotron Rad.* **12**, 374–379.
Gregory, B. W., Vaknin, D., Gray, J. D., Ocko, B. M., Cotton, T. M. & Struve, W. S. (1999). *J. Phys. Chem. B*, **103**, 502–508.
Gregory, B. W., Vaknin, D., Gray, J. D., Ocko, B. M., Stroeve, P., Cotton, T. M. & Struve, W. S. (1997). *J. Phys. Chem. B*, **101**, 2006–2019.
Gouy, A. (1910). *J. Phys. (Paris)*, **9**, 457–477.
Henke, B. L., Gullikson, E. M. & Davis, J. C. (1993). *Atom. Data Nucl. Data Tables*, **54**, 181–342.
Hunter, R. J. (1981). *Colloid Science.* London: Academic Press.
Israelachvili, J. (2000). *Intermolecular and Surface Forces.* London: Academic Press.
James, R. W. (1948). *The Optical Principles of the Diffraction of X-rays.* Ithaca, NY: Cornell University Press.
Kemner, K. M., Hunter, D. B., Elam, W. T. & Bertsch, P. M. (1996). *J. Phys. Chem.* **100**, 11698–11703.
Kjaer, K., Als-Nielsen, J., Helm, C., Tippman-Krayer, P. & Möhwald, H. (1989). *J. Phys. Chem.* **93**, 3200–3206.
Krestov, G. A., Novosyolov, N. P., Perelygin, L. S., Kolker, A. M., Safonova, L. P., Ovchinnikova, V. D. & Trostia, V. N. (1994). *Ionic Solvation*, ch. 5. New York: Ellis Horwood.
LeCalvez, E., Blaudez, D., Buffeteau, T. & Desbat, B. (2001). *Langmuir*, **17**, 670–674.
Luo, G., Malkova, S., Yoon, J., Schultz, D. G., Lin, B. H., Meron, M., Benjamin, I., Vanysek, P. & Schlossman, M. L. (2006). *Science*, **311**, 216–218.
McLaughlin, S. (1989). *Annu. Rev. Biophys. Chem.* **18**, 113–136.
Ninham, B. W. & Parsegian, V. A. (1971). *J. Theor. Biol.* **31**, 405–428.
Park, C., Fenter, P. A., Sturchio, N. C. & Regalbuto, J. R. (2005). *Phys. Rev. Lett.* **94**, 076104/1–4.
Parratt, L. G. (1954). *Phys. Rev.* **95**, 359–369.
Pittler, J., Bu, W., Vaknin, D., Travesset, A., McGillivray, D. J. & Losche, M. (2006). *Phys. Rev. Lett.* **97**, 046102/1–4.
Tajima, K. (1971). *Bull. Chem. Soc. Jpn*, **44**, 1767–1771.
Templeton, D. H., Templeton, L. K., Phillips, J. C. & Hodgson, K. (1980). *Acta Cryst.* A**36**, 436–442.
Travesset, A. & Vaknin, D. (2006). *Europhys. Lett.* **74**, 181–187.
Vaknin, D. (2001). *Methods in Materials Research*, edited by E. N. Kaufmann *et al.*, p. 10d.2.1–20. New York: Wiley.
Vaknin, D., Krüger, P. & Lösche, M. (2003). *Phys. Rev. Lett.* **90**, 178102/1–4.